

COMPUTATIONAL MODELING OF THE SQUIRREL-CAGE INDUCTION MOTOR STARTING PROCESS

Dr. Saleh Al-Jufout
Tafila Polytechnic,
Al-Balqa' Applied University,
P.O. Box 179, Tafila 66110, Jordan.
Tel.: +962.3.342326, Fax: +962.3.342327
E-mail: Tafil_cc@amra.nic.gov.jo

Abstract – This paper presents a methodology for computational modeling of the induction motor starting process. The numerical model of the squirrel-cage, three-phase induction motor is represented as a system of differential equations. The model takes in account the skin effect, transformation and rotational electromotive forces and it can give the instantaneous significant of required modes' parameters. The dynamic curves of the motor phase current, speed, active and reactive power and electromagnetic torque during starting process are obtained. The torque-speed and current-speed static characteristics are also obtained.

INTRODUCTION

In electric machinery course it is very essential to simulate some experiments that occur rapidly and might be dangerous or expensive, the necessity appears when performing them by students. Therefore, simulation enables students grasp the theoretical concepts of these experiments.

Motor starting process is one of the most important experiments in electrical engineering education, but it occurs within few seconds that makes it difficult to be observed. Simulation of this process permits to observe how the variables (current, torque and velocity) change during this process and compare different type of motors on the personal computer display.

Judged in terms of fitness for purpose coupled with simplicity, the induction motor must

rank alongside the screwthread as one of mankind's best inventions. It is not only supremely elegant as an electromechanical energy converter, but is also by far the most important, with something like one third of all the electricity generated being converted back to mechanical energy in induction motors. Despite playing a key role in industrial society, it remains largely unnoticed because of its workaday role in unglamorous surroundings driving machinery, pumps, fans, compressors, conveyors, hoists and a host of other routine but vital tasks. It will doubtless continue to dominate these fixed-speed applications, but thanks to the availability of reliable variable-frequency drives, it is also now will established in the controlled-speed arena.

Deep-bar or double-cage rotors of the induction motor have a high effective resistance at starting and a low effective resistance under normal running conditions, thus yielding both a high starting torque and good speed regulation in the same motor (Stephen J. Chapman 1991). Therefore, studying its dynamic and static characteristics is of a great importance.

THE NUMERICAL MODEL OF THE INDUCTION MOTOR

The numerical model of the three-phase, squirrel-cage induction motor is represented as a system of differential equations written in α , β rectangular coordinates (Jukov 1994).

To take in account the skin effect in the deep-

bar rotor of the induction motor, the squirrel-cage is represented as two resistive-inductive parallel connected circuits; consequently the numerical model, in matrix form, can be written as following:

$$L \frac{dI}{dt} = V - RI - \Omega LI$$

where

$$L = \begin{bmatrix} L_\alpha & 0 \\ 0 & L_\beta \end{bmatrix},$$

$$L_\alpha = L_\beta = \begin{bmatrix} L_S & L_\mu & L_\mu \\ L_\mu & L_R^{(1)} & L_\mu \\ L_\mu & L_\mu & L_R^{(2)} \end{bmatrix},$$

$$L_S = L_{\sigma S} + L_\mu,$$

$$L_R^{(1)} = L_{\sigma R} + L_\mu,$$

$$L_R^{(2)} = L_{\sigma R} + L_\mu,$$

$$R = \text{diag}[R_S, R_R^{(1)}, R_R^{(2)}, R_S, R_R^{(1)}, R_R^{(2)}],$$

$$\Omega = \begin{bmatrix} 0 & -\Omega_R \\ \Omega_R & 0 \end{bmatrix},$$

$$\Omega_R = \begin{bmatrix} 0 & 0 & 0 \\ 0 & -\omega & 0 \\ 0 & 0 & -\omega \end{bmatrix},$$

$$I = [\dot{i}_{S\alpha}, \dot{i}_{R\alpha}^{(1)}, \dot{i}_{R\alpha}^{(2)}, \dot{i}_{S\beta}, \dot{i}_{R\beta}^{(1)}, \dot{i}_{R\beta}^{(2)}]^T,$$

$$V = [v_{S\alpha}, 0, 0, v_{S\beta}, 0, 0]^T,$$

where

$\dot{i}_{S\alpha}, \dot{i}_{R\alpha}^{(1)}, \dot{i}_{R\alpha}^{(2)}, \dot{i}_{S\beta}, \dot{i}_{R\beta}^{(1)}, \dot{i}_{R\beta}^{(2)}$ – currents of the stator and equivalent rotor circuits in α, β coordinates respectively;

$v_{S\alpha}, v_{S\beta}$ – voltages applied to the terminals of the motor in α, β coordinates respectively;

$R_S, R_R^{(1)}, R_R^{(2)}$ – resistances of the stator and equivalent rotor circuits respectively;

$L_{\sigma S}, L_{\sigma R}^{(1)}, L_{\sigma R}^{(2)}, L_\mu$ – leakage inductances of the stator, equivalent rotor circuits and inductance of the magnetization branch respectively;

ω – angular velocity of the motor, which can be found by solving the following differential equation:

$$\frac{d\omega}{dt} = \frac{1}{J}(\tau - \tau_m),$$

where

J, τ, τ_m – the moment of inertia, electromagnetic torque and mechanical torque respectively.

The electromagnetic torque can be calculated as following:

$$\tau = \frac{1}{L_{\sigma S}} \left[\Psi_{S\beta} \sum_{i=1}^2 a_r^{(i)} \Psi_{R\alpha}^{(i)} - \Psi_{S\alpha} \sum_{i=1}^2 a_r^{(i)} \Psi_{R\beta}^{(i)} \right],$$

where

$$\Psi_{S\alpha} = L_{\sigma S} i_{S\alpha} + L_\mu \left(i_{S\alpha} + \sum_{i=1}^2 i_{R\alpha}^{(i)} \right),$$

$$\Psi_{S\beta} = L_{\sigma S} i_{S\beta} + L_\mu \left(i_{S\beta} + \sum_{i=1}^2 i_{R\beta}^{(i)} \right),$$

$$\Psi_{R\alpha}^{(i)} = L_{\sigma R}^{(i)} i_{R\alpha}^{(i)} + L_\mu \left(i_{S\alpha} + \sum_{i=1}^2 i_{R\alpha}^{(i)} \right),$$

$$\Psi_{R\beta}^{(i)} = L_{\sigma R}^{(i)} i_{R\beta}^{(i)} + L_\mu \left(i_{S\beta} + \sum_{i=1}^2 i_{R\beta}^{(i)} \right),$$

$$a_r^{(i)} = \frac{1}{L_{\sigma R}^{(i)}} \cdot \left[\frac{1}{L_{\sigma S}} + \frac{1}{L_\mu} + \sum_{k=1}^2 \frac{1}{L_{\sigma R}^{(k)}} \right]^{-1}.$$

The mechanical torque of the load, which is attached to the induction motor, can be considered either as a constant or as a function of the angular velocity. The active and reactive power of the motor can be calculated as following:

$$P = v_{s\alpha} i_{s\alpha} + v_{s\beta} i_{s\beta} ,$$

$$Q = v_{s\beta} i_{s\alpha} - v_{s\alpha} i_{s\beta} .$$

All the above mentioned differential equations can be solved by Runge-Kutta order four method. The voltages applied to the terminals of the induction motor are given as following:

$$v_{s\alpha} = V_m \cos \omega t ,$$

$$v_{s\beta} = V_m \sin \omega t .$$

The equivalent circuit parameters (resistances and inductances) can be defined in per units (*pu*) by engineering methods (Sivokobylenko and Kostenko 1979). The initial conditions of the variables (currents and angular velocity) equal to zero at the first step of solution.

EXPERIMENTAL RESULTS

The data below shows a comparison between a no-load starting process experiment and computational modeling results (the type of

the motor is AZ-12-52, 630 kW, 6 kV.), which confirms the scientific fulfillment of the developed numerical model:

	1*	2*
Duration of starting process, sec.	1.24	1.3
Starting current, <i>pu</i>	5.7	5.7
Dynamic inrush torque, <i>pu</i>	4.18	4.4
Starting torque, <i>pu</i>	1.17	1.2
Pullout torque, <i>pu</i>	1.8	1.9

1- computational modeling results. 2- experimental data.

RESULTS AND DISCUSSION

The developed numerical model permits to simulate the induction motor starting process and takes in account skin effect, transformation and rotational electromotive forces. In addition, this model is the same for both transients and steady-state analysis. Fig.1 shows the starting current (motor type: 2AZMP, 2500 kW, 6 kV), which is about five times greater the rated. Fig.2 shows the electromagnetic torque during the no-load starting process. The speed of the motor during starting process is shown in Fig.3. Fig.4 and Fig.5 show the consumed active and reactive power during the no-load starting process. As it is obvious, the reactive power is more than the consumed active power (the induction motor is running with a low power-factor) as there is no load attached to the motor.

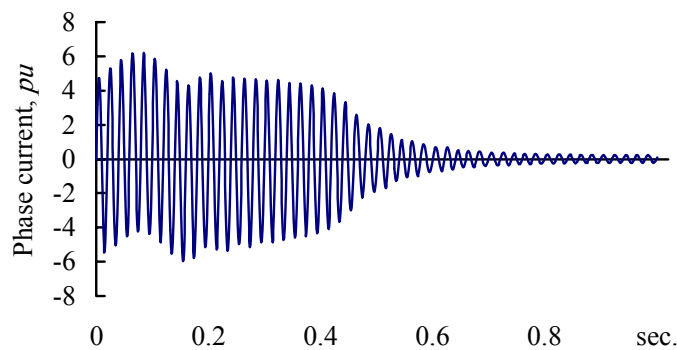


Fig.1- Induction motor phase current in *pu* during no-load starting process.

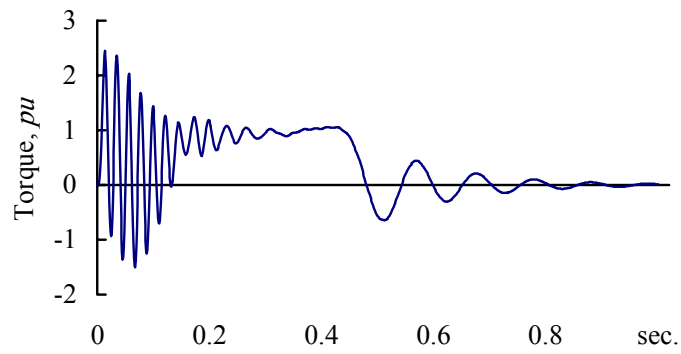


Fig.2- Induction motor torque in pu during no-load starting process.

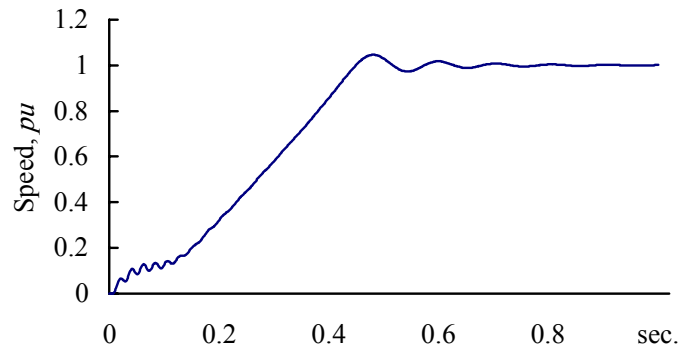


Fig.3- Induction motor speed in pu during no-load starting process.

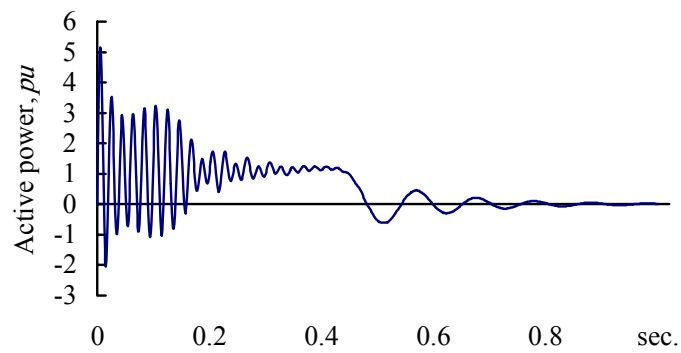


Fig.4- Induction motor active power in pu during no-load starting process.

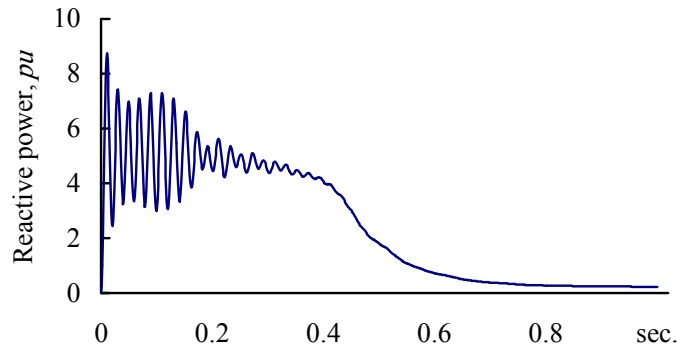


Fig.5- Induction motor reactive power in pu during no-load starting process.

Besides the dynamic characteristics, the torque-speed and the current-speed static characteristics can be achieved by using the developed model (Fig.6 and Fig.7 respectively), where it is shown that the starting torque is equal to $0.82 pu$ and the starting current is equal to $5.3 pu$.

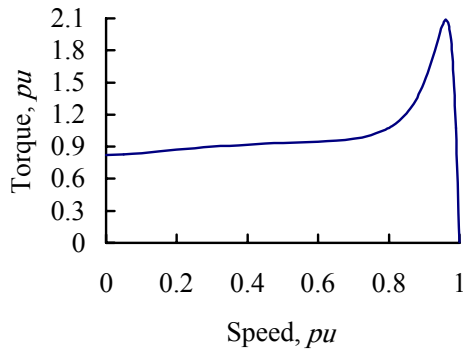


Fig 6- The torque-speed characteristic in pu .

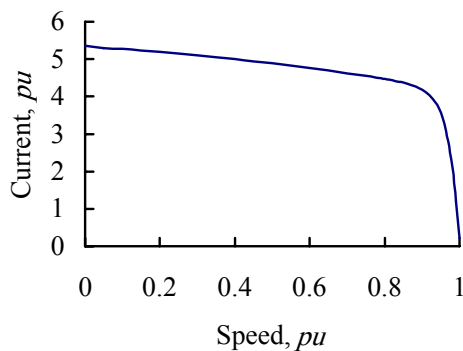


Fig.7- The current-speed characteristic in pu .

CONCLUSIONS

A numerical model has been developed to simulate the starting process of the three-phase, squirrel-cage induction motor. The developed model, which is represented as a system of differential equations, takes in account the skin effect, transformation and rotational electromotive forces. Using this model, starting process of the three-phase induction motor can be investigated. The skin effect has been taken in account by representing the rotor of the motor as two parallel-connected resistive-inductive circuits. Using the results of such numerical modeling, the optimum settings of relay protective devices and automates can be chosen and adjusted.

REFERENCES

- Jukov V.** 1994. *Short-circuit in electric system nodes with complex load*. MEI, Moscow.
- Sivokobylenko, V.; V. Kostenko.** 1979. *Electrical motors' mathematical modeling of the power station auxiliaries*. DPI, Donetsk.
- Stephen J. Chapman.** 1991. *Electric machinery fundamentals*. McGraw-Hill.